The Design of Low-power Conversion and Self-starting for Wireless Charging System

WENQIANG WEI, XIAODONG ZHUANG*
Electronic Information College
Qingdao University
Qingdao, China
wenqiangWei_01@163.com

Abstract: - The low-power conversion of voltage and the self-starting of the system based on wireless charging technology are studied. The system uses the XKT412 wireless charging module for wireless charging and uses super capacitors to store power. The system uses the MSP430F5529 single-chip microcomputer as the microprocessor to perform AD sampling on the charging circuit to realize the self-starting function of the circuit. The MSP430F5529 single-chip device performs the AD sampling of the voltage across the capacitor and sends the data to the OLED screen through the IIC communication mode for real-time display. The system outputs a voltage through a DC-DC converter circuit designed by the TPS63020 chip, and the ripple of the output voltage is less than 76mV. By designing a wireless charging car for experimental testing, the wireless charging efficiency of the system is higher than 85%. By using the MSP430F5529 single chip microcomputer and the TPS63020 chip, the power consumption of the system is effectively reduced and the function of automatically starting after charging is realized.

Key-Words: - wireless charging, low power consumption, MSP430F5529, TPS63020, self-starting, super capacitor, I^2C communication mode

1 Introduction

In recent years, the problems of air pollution and greenhouse effect have gradually increased, and the use of electric energy has been gradually extended to various fields. At present, the charging method of electronic products is divided into two methods: wired charging and wireless charging. In wired charging, frequent plugging and unplugging of the plug may cause problems such as aging of the socket and generation of electric sparks[1-4]. Damage to the wired charging line can cause safety hazards and poor adaptability to extreme weather[5-6]. The wireless charging technology solves the interface limitation and security problems of wired charging by getting rid of the limitation of the charging cable. Wireless charging transfers energy through electromagnetic induction, thus enabling static wireless efficient charging and dynamic charging of electronic products[7-8]. And wireless charging does not occupy the space on the ground, which brings great convenience. There are three main types of wireless charging technologies commonly used today: magnetic field coupling[9-10], electric field coupling[11-12], and electromagnetic radiation[13].

DC-DC technology is widely used in various electronic equipment fields. It is widely used in DC motor drive, uninterruptible power supply, aerospace power supply, and solar wind power generation. There are many DC conversion circuit topologies, the most basic ones are Buck and Boost circuits, and widely used such as flyback circuits. With the rapid development of electronic products, the conversion efficiency and power consumption requirements of DC-DC conversion circuits are also increasing[14-16]. For example, a DC-DC conversion chip must have a small size, a simple peripheral design circuit, and high stability[17-18].

This paper uses the case analysis method to design a wireless charging car as an example to realize the low power conversion of the wireless charging system and the self-starting function of the charging completion system.

2 System Composition

The system consists of two parts: a wireless charging transmitter and a wireless charging receiver. The system uses the MSP430F5529 single chip microcomputer as the micro-control processor of the wireless charging transmitter. The 5V/1A power supply is provided by the DC stabilized

* Xiaodong Zhuang is the corresponding author.

power supply for the single chip microcomputer and the XKT412 wireless charging module transmitting coil. The MSP430F5529 single chip microcomputer controls the on/off of the relay to realize the power-on and power-off of the wireless charging transmitter. The system block diagram is shown in Fig.1.

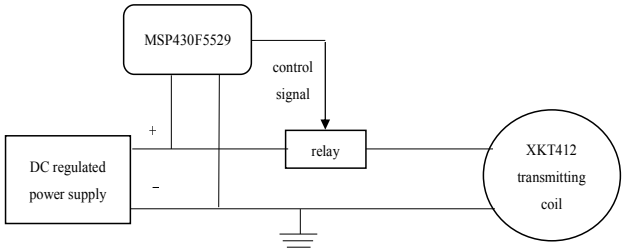

Fig.1 Wireless charging transmitter system block diagram

The system uses the MSP430F5529 single-chip microcomputer as the wireless charging receiver micro-control processor, and uses the super capacitor as the energy storage system. The wireless charging receiving end charges the super capacitor through the receiving coil of the XKT412 wireless charging module. When the voltage of the super capacitor reaches 1.8V of the working voltage of the TPS63020, the power of the super capacitor is stably outputted by the DC-DC conversion circuit to output the 5V voltage for the MSP430F5529 single chip and the system. The MSP430F5529 single-chip microcomputer starts normal operation and continuously samples the wireless charging receiving coil and the capacitor voltage. The OLED screen displays the voltage across the capacitor in real time. When the voltage of the wireless charging receiving coil is 0 or the voltage across the capacitor is equal to Vcc, the MSP430F5529 single-chip microcomputer starts the system operation. The block diagram of the wireless charging receiver system is shown in Fig.2.

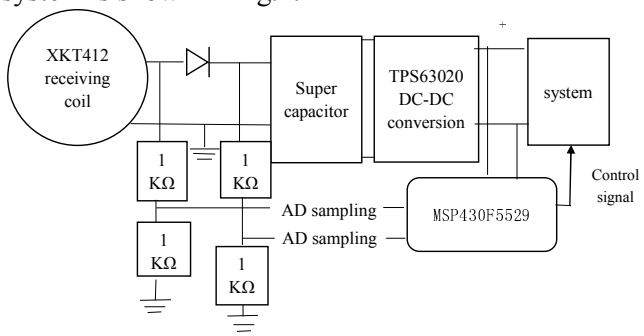

Fig.2 Wireless charging receiver system block diagram

3 Subsystem Design

3.1 Wireless Charging System

3.1.1 The of Advantages of the XKT412 Wireless Charging Module

In order to achieve high efficiency wireless charging, the wireless charging module must be required to have high current and high power utilization. The XKT412 wireless charging module has a simple circuit. The maximum charging current that can be obtained under the 5V/1A power supply is >0.85A, and the energy utilization rate is extremely high.

3.1.2 The Spacing between the Charging Coil and the Receiving Coil

When the power supply of 5V/1A is supplied, the experimental data of the charging current when the voltage across the capacitor U<0.9Vcc is measured by changing the interval between the charging coil and the receiving coil is shown in Table 1.

Table 1 Relationship between power utilization efficiency of charging coil and coil spacing

Coil spacing	1 mm	2 mm	3 mm	4 mm	5 mm
Voltage and current supplied	5V 1A	5V 1A	5V 1A	5V 1A	5V 1A
Charging voltage	5V	5V	5V	5V	5V
Charging current	0.67A	0.86A	0.86A	0.56A	0.2A
Power utilization efficiency	67%	86%	86%	56%	20%

By measuring the experimental data, when the charging coil and the receiving coil are separated by 2~3mm, the electric energy utilization rate of the XKT412 wireless charging module can reach more than 85%, and the electric energy utilization rate is extremely high.

3.2 Energy Storage System

3.2.1 Super Capacitor Breakdown Voltage

Since the power supply voltage is 5V, in order to prevent the breakdown capacitance when the capacitor is charged, the system selects a super

capacitor with a breakdown voltage of 5V to store the electric energy.

3.2.2 Super Capacitor Capacity

According to the capacitor charge and discharge formula[19]:

$$U(t) = Vcc(1 - e^{\frac{-t}{RC}}) \quad (1)$$

When the capacitor voltage U = 0.9 Vcc, t = ln10 RC ≈ 2.3 RC. After measurement, the wireless charging receiving end circuit resistance R ≈ 2.5 Ω. In order to reduce the test time, the system selects 10F super capacitor for experimental test, that is, the capacity can be charged to 4.5V when t≈57.5s.

3.3 DC-DC System Chip Selection

3.3.1 LM2596S Chip

LM2596S chip can realize voltage drop and output voltage stability[20-22]. However, LM2596S chips have high calorific value and are not suitable for low power systems. Moreover, the corresponding circuit parameters must be modified for different input voltages, so it is not suitable for DC-DC converter with time-varying input voltages. The LM2596S pin diagram is shown in Fig.3.

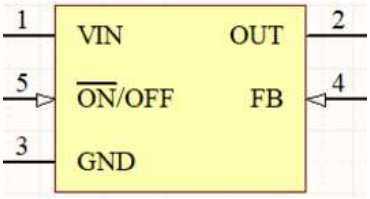

Fig.3 LM2596S pin diagram

3.3.2 TPS63020 Chip

The efficiency of TI's TPS63020 chip is as high as 96%. It can automatically change the step-up and step-down mode. Its input voltage range is wide (1.8-5.5V). Its output voltage is adjustable in the range of 1.2-5.5V. Its static current is small and it has the advantages of over-temperature and over-voltage protection. Moreover, when the circuit parameters are fixed, the output voltage will not change with the change of the input voltage. The TPS63020 pin diagram is shown in Fig.4.

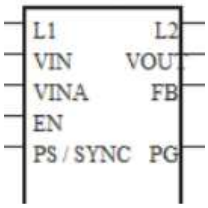

Fig.4 TPS63020 pin diagram

3.4 DC-DC Conversion Circuit

The DC-DC conversion circuit is based on TI's TPS63020EVM. Based on this, the inductor is modified to reduce the interference of the circuit and the layout is adjusted to reduce the interference of the circuit.

Adjusting the ratio of the resistance across the feedback port FB changes the output voltage. According to the TPS63020 data sheet:

$$R_1 = R_2\left(\frac{V_{OUT}}{V_{FB}} - 1\right) \quad (2)$$

And the system sets the output voltage Vout=5V, R_2=200Ω, and calculates R1=1.8MΩ. The schematic diagram of the DC-DC converter circuit is shown in Fig.5. The layout of the PCB component of the DC-DC converter circuit is shown in Fig.6.

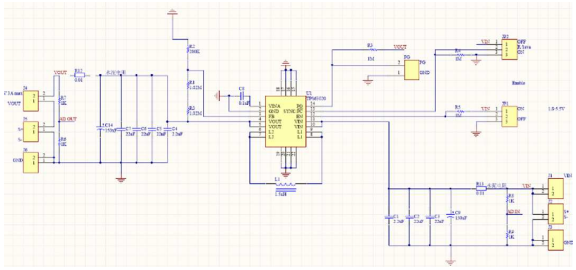

Fig.5 DC-DC conversion circuit schematic

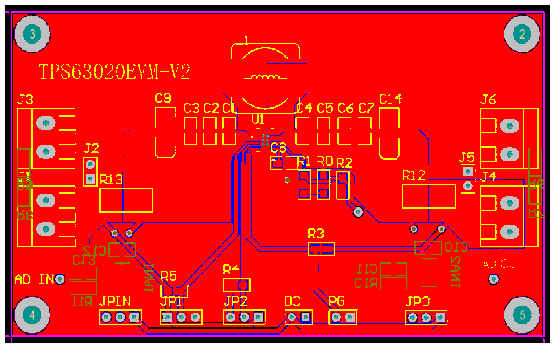

Fig.6 DC-DC converter circuit PCB component layout

The output voltage is measured by an oscilloscope and the output voltage ripple is less than 76mV.

3.5 Selection of Single Chip Microcomputer

3.5.1 STC89C52 Microcontroller

The 51 series of single-chip microcomputers are widely used. From internal hardware to software, there is a complete set of bit-wise operating systems. The processing object is not a byte but a bit. Not only can certain bits of some special function registers be processed, such as transfer, set, clear, test, etc., but also bit logic operations[23]. However, the operation speed is slow and the power consumption is high. When used in conjunction with the LCD1602 liquid crystal panel, the circuit becomes complicated, and the overall performance of the system is degraded. The pin diagram of STC89C52 microcontroller is shown in Fig.7.

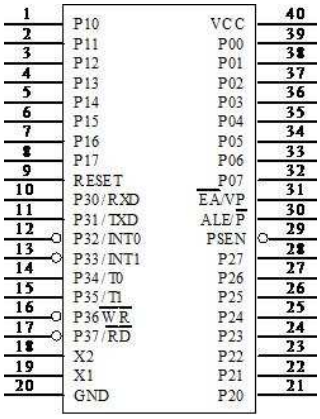

Fig.7. Pin Diagram of STC89C52 Microcontroller

3.5.2 STM32 Microcontroller

STM32 MCU is a series of single-chip microcomputer with high cost performance. It has powerful computing functions and first-class peripherals[24]. However, it is inferior to MSP430 series MCU in terms of power consumption, which is not suitable for the low power requirements of this system. The pin diagram of STM32F103xx MCU is shown in Fig.8.

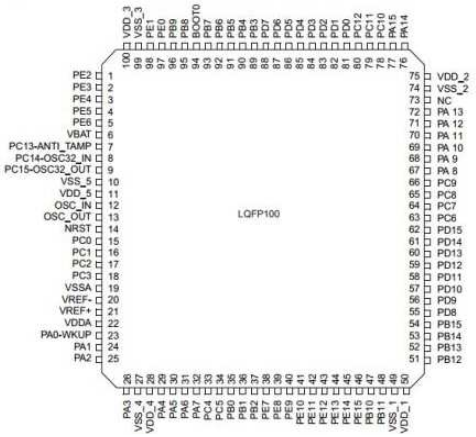

Fig.8.Pin Diagram of STM32F103xx MCU

3.5.3 MSP430F5529 Microcontroller

MSP430F5529 is a 16-bit ultra-low power microcontroller with 128KB flash memory, 8KB SRAM, 63 programmable I/O ports, 4 16-bit timers/counters, abundant interrupt sources, etc[25]. It has a wide range of low-power mode combinations, suitable for battery-powered products, and it is a compact instruction set (RISC) structure, powerful, resource-rich on-chip, fast operation, and the microcontroller is small, light weight, for low-power system has obvious advantages[26]. And it is very simple to design display circuit by I^2C communication mode. The pin diagram of the MSP430F5529 microcontroller is shown in Fig.9.

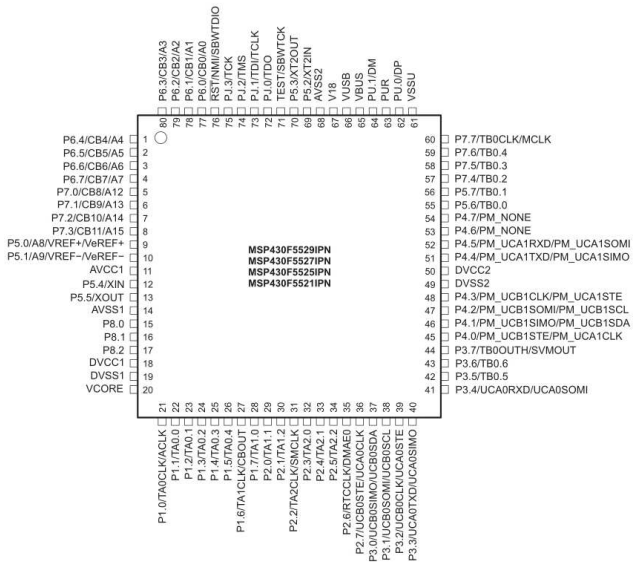

Fig.9. Pin Diagram of MSP430F5529 Microcontroller

Considering that the system is designed to achieve simple display circuit and low power consumption, the MSP430F5529 microcontroller is used as the central control chip.

3.6 Selection of Display

3.6.1 LCD Display

LCD display is a liquid crystal screen, which can not emit light itself[27]. It needs backlight to control the angle of liquid crystal through an external circuit through the liquid crystal layer. LCD display has the advantages of simple process, high cost performance, and stable and controllable image of large layout. But LCD display has high energy consumption, small viewing angle, low pass rate and complex peripheral circuit[28-29]. The physical picture of LCD1602 display screen is shown in Fig.10.

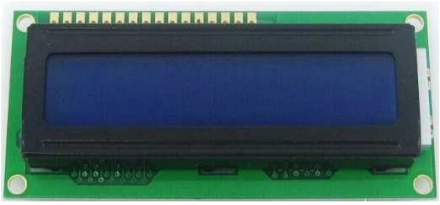

Fig.10. Physical picture of LCD1602 display screen

3.6.2 OLED Display

OLED can emit its own light without backlight, which can be directly presented by tricolor technology[30-31]. OLED display has brighter imaging, wider viewing angle, low energy consumption, and data transmission can be carried out through I^2C communication mode. The peripheral circuit design is simple. The physical picture of OLED display screen is shown in Fig.11.

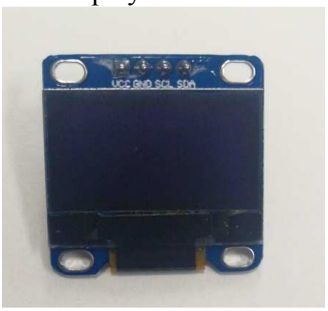

Fig.11. Physical picture of OLED display screen

Considering the simple design and low power consumption of the peripheral circuit of OLED display screen, the system uses OLED display screen to display the sampling voltage in real time.

4 I^2C Communication Mode

4.1 Advantages of I^2C Bus

(1) I^2C has two bus lines, a serial data line SDA and a serial clock line SCL.
(2) Each device connected to the bus has a unique address.
(3) The bit rate of serial 8-bit bidirectional data transmission can reach 100 kbits/s in standard mode, 400 kbits/s in fast mode and 3.4 Mbits/s in high-speed mode.
(4) Support multiple master modules, but only one master is allowed at the same time.

4.2 I^2C Bus Protocol

Bus can start data transmission only when it is not busy. The schematic diagram of data transmission of "start" and "stop" shows that when SCL line is high level, SDA line will be "start" from high level to low level, and all data transmission must have "start" condition. When SCL line is high level, SDA line will be "stop" condition from low level to high level. All data transmission must end with a "stop" condition. The SCL and SDA lines remain at high levels during this period to indicate idle state after the "stop" condition and before the "start" condition[32]. The timing diagram of the I^2C protocol start and end conditions is shown in Fig.12.

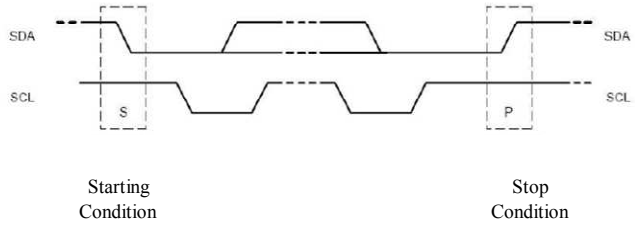

Fig.12. Timing diagram of I^2C protocol start and end conditions

The I^2C bus data data transmission is in byte format, that is, each byte sent to the SDA line must be 8 bits, the highest bit (MSB) is transmitted first, and each transmitted byte must be followed by a response bit (Issued by the slave). All masters generate their own clocks on the SCL line to transmit messages on the I^2C bus. The data is valid only during the high period of the clock. When transmitting data, the SDA line must be stable during the high period of the SCL line. The high or low state of the SDA can only be changed when the SCL line is low. A deterministic clock is required for bitwise arbitration. The I^2C bus addressing mode is clearly defined. The 7-bit addressing mode is adopted. The highest byte of the first byte transmitted indicates the slave address, and the lowest bit (the 8th LSB) determines the data transmission direction. If it is '0'. Indicates that the host writes data to the slave. If it is '1', the host reads data from the slave. When an address is sent, each device in the system compares the first 7 bits with its own address after the start condition. If so, the device will determine that it is addressed by the host.

5 Self-starting Function Principle

The system can trigger the self-starting function in two situations. The first one is to power off the wireless charging transmitter, and the other is to reach the Vcc of the super capacitor voltage.

5.1 Hardware Circuit

The MSP430F5529 single chip microcomputer determines whether self-starting is performed by separately sampling the voltage across the capacitor and the voltage across the receiving coil of the XKT412 wireless charging module. The system uses a diode to separate the XKT412 wireless charging receiving coil and the super capacitor. The positive pole of the diode is connected to the output coil of the XKT412 wireless charging module, and the negative pole of the diode is connected to the super capacitor. Therefore, the voltage U1 of the positive terminal of the diode is the receiving coil voltage of the XKT412 wireless charging module. The diode negative terminal voltage U2 is the voltage of the capacitor. In order to prevent the AD sampling voltage from penetrating the MSP430F5529, the system uses two 1KΩ resistors for voltage division sampling. When the sampling voltage of the positive terminal of the diode is 0 or the voltage of the negative terminal of the diode is Vcc/2, the MSP430F5529 starts the system. The sampling principle is shown in Fig.13.

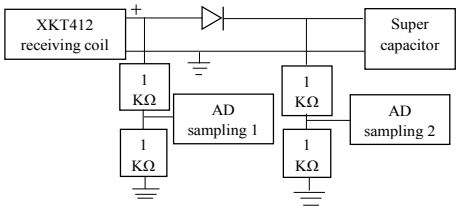

Fig.13 Sampling schematic

5.2 Software Programming

After the microcomputer is powered, the voltage sampling is continued. To prevent the judgment error, the MCU starts the system operation when the self-start condition is satisfied for 5 consecutive times. The MCU stops the AD sampling 1 and enters the low power state. The block diagram is shown in Fig 14.

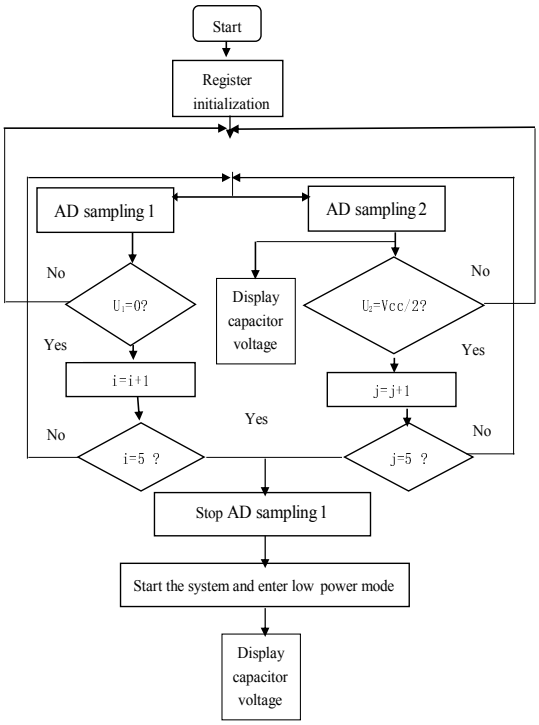

Fig.14 Block diagram

6 System Debugging

First discharge all the energy in the capacitor. The wireless charging receiving coil is mounted on the electric cart and is 2.5 mm from the wireless charging transmitting coil. The wireless charging transmitter is provided with a 5V/1A power supply, and the single-chip driving relay of the wireless charging transmitting end is energized to supply power to the wireless charging transmitting coil. The wireless charging receiving coil starts to charge the super capacitor. When the voltage across the capacitor reaches 1.8V, the DC-DC converter circuit stably outputs 5V voltage and the ripple is less than 76mV. The wireless charging receiver starts working, and the voltage across the capacitor is displayed in real time on the OLED. Displayed on the screen. When the voltage across the capacitor is equal to 5V, the wireless charging receiver detects the charging and drives the car to drive and displays the voltage across the capacitor in real time.

Discharge all the power in the capacitor again. The wireless charging transmitter terminal is timed for 50s. When the charging starts, the wireless charging transmitter transmits the power to the wireless charging transmitting coil. The wireless charging receiving coil starts to charge the super capacitor. When the voltage across the capacitor reaches 1.8V, the DC-DC converter circuit stably outputs 5V voltage and the ripple is less than 76mV. The wireless charging receiver starts working, and the voltage across the capacitor is displayed in real time on the OLED. Displayed on the screen. After

the charging of 50s, the single-chip drive relay of the wireless charging transmitting end is disconnected, and the single-chip microcomputer of the wireless charging receiving end detects that the charging car is driven after the end of charging and displays the voltage across the capacitor in real time.

7 Conclusion

The system uses a 5V/1A power supply to wirelessly charge the super capacitor. When the wireless charging transmitting coil is separated from the wireless charging receiving coil by 2~3mm, the wireless charging efficiency is greater than 85%. The super capacitor is discharged by the DC-DC converter circuit designed by the TPS63020 chip. The input voltage range is wide, the output voltage is stable at 5V, and the peak-to-peak value of the voltage fluctuation is less than 76mV. The system effectively reduces the power consumption of the system by using the MSP430F5529 microcontroller and the TPS63020 chip. The wireless charging technology effectively improves the service life and safety of the charging device of the system. The stability of the output voltage of the system ensures the stability of the operation of the electronic product. If the system is applied to electronic products such as sweeping robots, the stability of the products will be further improved, and the self-starting function will further improve the performance of the products.

References:

[1] Philip Machura, Quan Li, A critical review on wireless charging for electric vehicles, *Renewable and Sustainable Energy Reviews*, Vol.104, April 2019, pp. 209-234.

[2] Young Dae Ko, Young Jae Jang, Efficient design of an operation profile for wireless charging electric tram systems, *Computers & Industrial Engineering*, Vol.127, January 2019, pp. 1193-1202.

[3] Young Jae Jang, Survey of the operation and system study on wireless charging electric vehicle systems, *Transportation Research Part C: Emerging Technologies*, Vol.95, October 2018, pp. 844-866.

[4] Sotiris Nikoletseas, Theofanis P. Raptis, Christoforos Raptopoulos,Wireless charging for weighted energy balance in populations of mobile peers, *Ad Hoc Networks*, Vol.60, May 2017, pp. 1-10.

[5] Kafeel Ahmed Kalwar, Muhammad Aamir, Saad Mekhile, A design method for developing a high misalignment tolerant wireless charging system for electric vehicles, *Measurement*, Vol.118, March 2018, pp. 237-245.

[6] Zicheng Bi, Lingjun Song, Robert De Kleine, Chunting Chris Mi, Gregory A. Keoleian, Plug-in vs. wireless charging: Life cycle energy and greenhouse gas emissions for an electric bus system, *Applied Energy*, Vol.146,15 May 2015, pp. 11-19.

[7] Chirag Panchal, Sascha Stegen, Junwei Lu, Review of static and dynamic wireless electric vehicle charging system, *Engineering Science and Technology* ,Vol.21, No.5, October 2018, pp. 922-937.

[8] Carlos A. García-Vázquez, Francisco Llorens-Iborra, Luis M. Fernández-Ramírez, Higinio Sánchez-Sainz, Francisco Jurado,Comparative study of dynamic wireless charging of electric vehicles in motorway, highway and urban stretches, *Energy*, Vol.137, October 2017, pp. 42-57.

[9] Kurs A,Karalis A,Moffatt R, Wireless powertransfer via strongly coupled magnetic resonances,*Science*, Vol.317, No.5834, 2007, pp. 83-86.

[10] Karalis A, Joannopoulos J D, Soljacicm,Efficient wireless non-radiative mid-range energy transfer, *Annals of Physics*, Vol.323, No.1, 2008, pp. 34-48.

[11] Ludois D C,Reed J K,Hanson K,Capacitive powertransfer for rotor field current in synchronous machines, *IEEE Transactions on Power Electronics*, Vol.27, No.11,2012, pp. 4638-4645.

[12] Liu C,Hu A P,Nair N K C,Modelling and analysis of acapacitively coupled contactlesspower transfer system,*IET Power Electronics*, Vol.4, No.7, 2011, pp. 808-815.

[13] Lin J C,Space solar-power stations,wireless power transmissions,and biological implications,*IEEE Microwave Magazine*, Vol.3, No.1, 2002, pp. 36-42.

[14] Ram Krishan, Ashu Verma, Sukumar MishraL,Loadability analysis of DC distribution systems, *International Journal of Electrical Power & Energy Systems*, Vol.103, 2018, pp. 176-184.

[15] Tarek Youssef,Moataz Elsied, A.Salem, Amrane Oukaour, Osama Mohammed,Carrier extraction based synchronization scheme for distributed DC–DC converters in DC-

Microgrid, *Electric Power Systems Research*, Vol.161, 2018, pp. 114-122.

[16] Driss Oulad-Abbou, Said Doubabi, Ahmed Rachid, Power switch failures tolerance of a photovoltaic fed three-level boost DC-DC converte, *Microelectronics Reliability*, Vol.92, January 2019, pp. 87-95.

[17] Elham Kordetoodeshki, Alireza Hassanzadeh, An ultra-low power, low voltage DC-DC converter circuit for energy harvesting applications, A*EU-International Journal of Electronics and Communications*, Vol.98, January 2019, pp. 8-18.

[18] Taha Ahmadi, Esmaeel Rokrok, Mohsen Hamzeh,Supervisory control of bipolar DC microgrids equipped with three-port multidirectional DC–DC converter for efficiency and system damping optimization, *Sustainable Energy*, Vol.16,December 2018, pp. 327-340.

[19] Ottorino Veneri, Clemente Capasso, Stanislao Patalano,Experimental investigation into the effectiveness of a super-capacitor based hybrid energy storage system for urban commercial vehicles, *Applied Energy*,Vol.227,October 2018, pp. 312-323.

[20] Han Fei ,Yang Fang, Wang Yang ,Duan Minghui ,Peng Lizhi, Li Youze, Study on Adjustable DC Magnetic Seed Treatment Equipment, *Journal of Agricultural Mechanization Research*, Vol.9,2014, pp. 85-88.

[21] LI Wentao ,LI Ruigang, Design of SSI Interface Module for Communication Based on FPGA, *Control and Instruments in Chemical Industry*, Vol.45, 2018, pp. 324-328.

[22] Zhao Qing ,Ding Guangzhe, The Design of Metal Object Detection Locator Based on LDC1000, *Bulletin of Science and Technology*, Vol.33, 2017, pp. 90-93.

[23] Tianhu Wang, Tianyu Chen, Yue Hu, Xiaoyong Zhou, Naiping Song, Design of intelligent LED lighting systems based on STC89C52 microcomputer, *Optik*, Vol.158, April 2018, pp. 1095-1102.

[24] Huifu Zhang, Wei Kang, Design of the Data Acquisition System Based on STM32, *Procedia Computer Science*, Vol.17, 2013, pp. 222-228.

[25] Hyosang Yoon, Xing Xuan, Sungkwan Jeong, Jae Y. Park ,Wearable, robust, non-enzymatic continuous glucose monitoring system and its in vivo investigation, *Biosensors and Bioelectronics*,Vol.117,October 2018, pp.267-275.

[26] Pinwei Zhu, Chunhua Hu, Design of Wireless Electronic Scale Based On MSP430 Microprocessor, *AASRI Procedia*, Vol.1, 2012, pp. 581-587.

[27] Kyung Joon Kwon, Min Beom Kim, Cheon Heo, Seong Gyun Kim, Young Hwan Kim, Wide color gamut and high dynamic range displays using RGBW LCDs, *Displays*, Vol.40, December 2015, pp. 9-16.

[28] C. Alejandro Parraga, Jordi Roca-Vila, Dimosthenis Karatzas, Sophie M. Wuerger,Limitations of visual gamma corrections in LCD displays, *Displays*, Vol.35, No.5, December 2014, pp. 227-239.

[29] Kaida Xiao, Chenyang Fu, Dimosthenis Karatzas, Sophie Wuerger,Visual gamma correction for LCD displays, *Displays*, Vol.32, No.1, January 2011, pp. 17-23.

[30] Yonghun Choi, Rhan Ha, Hojung Cha, Fully automated OLED display power modeling for mobile devices, *Pervasive and Mobile Computing*, Vol.50, October 2018, pp. 41-55.

[31] Jong-Kwon Lee, Seunghyun Cho, Dong Wan Kang,Analysis of light leakage between the adjacent pixels in a color-filter stacked white OLED display, *Displays*, Vol.45, December 2016, pp. 6-13.

[32] Dai Jiejie, Song Hui, The IIC interface based on ATmega8 realizes the applications of PS/2 keyboard/mouse in the system, *Procedia Engineering*, Vol.16, 2011, pp. 673-678.